

International Journal of Bifurcation and Chaos, Vol. 31, No. 13 (2021) 2150203 (14 pages) © World Scientific Publishing Company

DOI: 10.1142/S0218127421502035

Modeling the Effect of Reactive Oxygen Species and CTL Immune Response on HIV Dynamics

Qi Deng* and Ting Guo[†]

Department of Mathematics,

Nanjing University of Science and Technology,

Nanjing, Jiangsu 210094, P. R. China

*dddengqiaaa@163.com

[†]gtnjust@163.com

Zhipeng Qiu[‡]

Center for Basic Teaching and Experiment, Nanjing University of Science and Technology, Jiangyin, Jiangsu 214443, P. R. China smoller_1@163.com

Libin Rong

Department of Mathematics, University of Florida, Gainesville, FL 32611, USA libinrong@ufl.edu

Received; Revised

Individuals infected by human immunodeficiency virus (HIV) are under oxidative stress due to the imbalance between reactive oxygen species (ROS) production and elimination. This paper presents a mathematical model with the cytotoxic T lymphocytes (CTL) immune response to examine the role of ROS in the dynamics of HIV infection. We classify the equilibria of the model and study the stability of these equilibria. Numerical simulations show that incorporating ROS and CTL immune response into the model leads to very rich dynamics, including bistable phenomena and periodic solutions. Although the current antiretroviral therapy can suppress viral load to the undetectable level, it cannot eradicate the virus. A high level of ROS may be a factor for HIV persistence in patients despite suppressive therapy. These results suggest that oxidative damage and anti-oxidant therapy should be considered in the study of HIV infection and treatment.

Keywords: HIV; Reactive Oxygen Species (ROS); bistability; oxidative stress.

1. Introduction

HIV, the pathogen leading to the acquired immunodeficiency syndrome (AIDS), is highly aggressive to the human immune system. The impaired immune system in untreated HIV patients can no longer fight against opportunistic infections that are normally not problematic [Nowak & May, 2000]. The most recent Global Health Observatory (GHO) data of HIV/AIDS published by WHO estimates that there were approximately 38.0 million people living with HIV at the end of 2019 and around 33 million people have died of HIV since the beginning

[‡]Author for correspondence

of the epidemic WHO, 2020. This emphasizes the need for further research on HIV infection and

Mathematical models have proven to be a useful tool for studying HIV dynamics [Rong & Perelson, 2009; Rong et al., 2007b; Guo et al., 2020a; Sun et al., 2018; Feng & Qiu, 2019; Feng et al., 2019. Over the past two decades, many modeling studies have been conducted to investigate HIV infection Guo et al., 2020b; Allali et al., 2017; Souza & Zubelli, 2011; Deng *et al.*, 2021; Guo & Qiu, 2019; Lv et al., 2014. Perelson and Nelson 1999 used a three-dimensional ordinary differential equations (ODE) model to describe the interaction between the viruses and the host cells. This basic viral dynamic model includes three variables: uninfected CD4+ T cells, productively infected CD4+ T cells, i.e. infected CD4+ T cells that can produce new virions, and free viruses. Rong et al. 2007c developed a four-dimensional ODE model including unproductively infected cells that cannot produce new virions, i.e. infected CD4+ T cells in the eclipse stage (the stage of an infected cell between viral attachment and generation of new virus). During HIV infection, cytotoxic T lymphocytes (CTL) are a major component of the immune response against viral infection Guo & Qiu, 2019. Maziane et al. [2017] studied a class of mathematical models with unproductively infected cells and CTL immune response, and showed the critical role of CTL immune response in controlling HIV infection.

Most of the above models do not consider the effect of reactive oxygen species (ROS) on HIV infection. Mounting biological studies indicate that long-term HIV infection may result in the accumulation of ROS Pace & Leaf, 1995; Schwarz, 1996; Tang & Smit, 2000. ROS are the by-products of cellular respiration, and play an important role in cell signaling Hildeman, 2004; Gil et al., 2003; Yang et al., 2020. ROS promote the aging of the body and cause various diseases although ROS can assist the body in resisting and killing bacteria and other pathogens. In a healthy body, the natural defense system (e.g. enzyme system; antioxidants) can eliminate the toxic effects of ROS. Thus, the process of producing ROS and detoxication can reach a dynamic balance. However, in HIV patients, this balance is disturbed due to a high serum concentration of ROS and a low antioxidant concentration Schwarz, 1996; Flores et al., 1993.

The resulting oxidative stress affects the progression of HIV in several ways, such as destroying the immune response to HIV and promoting viral replication Pace & Leaf, 1995; Stephensen et al., 2005. Therefore, in order to control HIV infection, it is necessary to understand the role of ROS in HIV dynamics.

A couple of mathematical models including ROS have also been developed to study HIV dynamics. van Gaalen and Wahl [2009] constructed a four-dimensional ODE model to evaluate the relationship between ROS and antioxidants, and to estimate model parameters using clinical data. Although many infected individuals exhibit sustained low-level viremia on ART, a number of them have occasional viral load measurements above the detection limit (50 copies/mL). Such transient episodes of detectable viremia are termed "viral blips". Zhang et al. [2013] reanalyzed the model in van Gaalen & Wahl, 2009 and proposed that considering ROS might contribute to the occurrence of viral blips. Wang et al. 2018 investigated a withinhost model of HIV infection with impaired immune function caused by oxidative stress. They obtained several thresholds for virus rebound and highlighted the importance of the CTL immune response.

Motivated by the work of Rong et al. 2007c and van Gaalen and Wahl [2009], we developed an HIV infection model with the CTL immune response and ROS. The model is shown schematically in Fig. I and described by the following system of ODE

$$\begin{cases}
\frac{\mathrm{d}T(t)}{\mathrm{d}t} = \lambda - dT - (1 - \varepsilon)\beta(I)TI + \alpha E, \\
\frac{\mathrm{d}E(t)}{\mathrm{d}t} = (1 - \varepsilon)\beta(I)TI - (d_E + \alpha + \pi)E, \\
\frac{\mathrm{d}I(t)}{\mathrm{d}t} = \pi E - \delta I - pIZ, \\
\frac{\mathrm{d}Z(t)}{\mathrm{d}t} = cIZ - bZ,
\end{cases} \tag{1}$$

where T(t), E(t), I(t) and Z(t) denote uninfected CD4+ T cells, infected CD4+ T cells in the eclipse stage, productively infected CD4+ T cells, and CTL immune response at time t, respectively. Following the definition in Shiri et al., 2005, the unit of T(t), E(t), I(t), and Z(t) should be mL^{-1} .

Effect of Reactive Oxygen Species and CTL Immune Response on HIV Dynamics

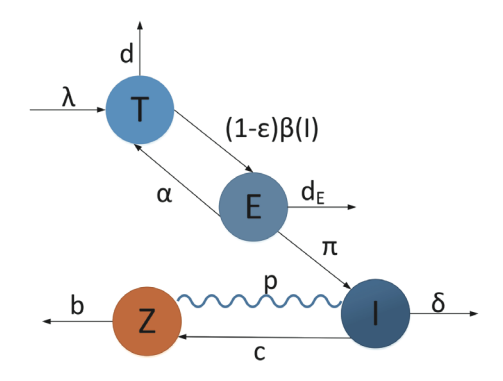


Fig. 1. The schematic diagram of HIV transmission. The wavy line is used to emphasize the killing effect of the CTL immune response on productively infected cells.

The parameter λ is the generation rate of uninfected CD4+ T cells and d is the death rate. The effectiveness of drug therapy is ε . Infected cells in the eclipse stage can revert to the uninfected state at a rate α . They become productive at the rate π and die at the rate d_E . Productively infected cells die naturally at a rate δ and are removed by the CTL immune response at a rate p. The term cIZ is the generation rate of CTLs in response to antigenic stimulation and b is the clearance rate of CTLs.

As stated in the document Gloire et al., 2006, ROS can enhance HIV replication through the activation of transcription factor NF-kB. During HIV infection, productively infected cells indirectly

produce a high level of ROS Pace & Leaf. 1995: Schwarz, 1996, which in turn increases virus production and promotes HIV infection. Thus, we use productively infected cells to affect the infection rate to capture ROS-activated transcription in our model. Based on the above discussion, the infection rate $\beta(I)$ should have the following properties for I: (1) $\beta(I) > 0$; (2) $\frac{d\beta(I)}{dI} > 0$. Specifically, we take

$$\beta(I) = b_0 + \frac{I(b_1 - b_0)}{I + b_2}. (2)$$

Obviously, $\beta(I)$ satisfies the properties (1) and (2). In fact, such saturation function can effectively limit the infection rate to the maximum value (b_1) at the high level of I, which is more realistic. Here, b_0 represents the infection rate in the absence of ROS, while b_1 denotes the maximum infection rate, and b_2 is the density of productively infected cells when the infectivity takes its median value. We regard b_1 as an oxidant parameter in the numerical investigations performed later. This infectivity has been introduced in Zhang et al., 2014; van Gaalen & Wahl, 2009. The detailed description and values of the parameters are listed in Table 1

It is noted that model (1) did not include the dynamics of free viruses explicitly. The turnover of free viruses is much faster than that of productively infected cells Bartholdy et al., 2000. This

Table 1. Parameter descriptions and sources for their values.

Parameter	Value	Description	Reference
λ	$10^4 \mathrm{mL}^{-1} \mathrm{day}^{-1}$	Production rate of uninfected cells	[Rong et al., 2007c]
d	$0.01{\rm day}^{-1}$	Death rate of uninfected cells	[Perelson et al., 1993]
α	$0.01\mathrm{day}^{-1}$	Rate of infected cells in the eclipse stage reverting to the uninfected state	[Rong et al., 2007c]
d_E	$0.7\mathrm{day}^{-1}$	Death rate of infected cells in the eclipse stage	[Rong et al., 2007c]
π	$1.1\mathrm{day}^{-1}$	Rate of infected cells in the eclipse stage progressing to the productive stage	[Rong et al., 2007c]
δ	$1\mathrm{day}^{-1}$	Death rate of infected cells	[Rong et al., 2007a]
b_0	$2.5 \times 10^{-8} - 5 \times 10^{-4} \mathrm{mL day}^{-1}$	Infection rate in the ROS-absent case	[Wang et al., 2009]
b_1	$2.5 \times 10^{-6} - 5 \times 10^{-2} \mathrm{mL day}^{-1}$	Maximum infection rate or the oxidant parameter	See text
b_2	$0.0001 - 0.1 \mathrm{mL}^{-1}$	Infected cell concentration when the infectivity takes its median value	See text
p	$0.002 \mathrm{day}^{-1}$	Clearance rate of infected cells by CTL killing	[Shiri et al., 2005]
c	$0.00001 - 0.1 \mathrm{mL}^{-1} \mathrm{day}^{-1}$	Generation rate of CTL	[Wang et al., 2012; Wodarz & Lloyd, 2004]
b	$0.1\mathrm{day}^{-1}$	Death rate of CTL	[Shiri et al., 2005; Wodarz & Lloyd, 2004]
ε	0-1	Efficacy of drug therapy	See text

Q. Deng et al.

allows us to make a quasi steady-state assumption, i.e. the concentration of free viruses is simply proportional to the concentration of productively infected cells [Wodarz et al.], 2002]. As stated in biological documents Pace & Leaf, 1995; Stephensen et al., 2005, a high concentration of ROS is beneficial to HIV disease by promoting the replication of viruses, decreasing the proliferation of immune cells and increasing the sensitivity to drug toxicities, etc. However, it is challenging to include all biological details in a modeling work. In this paper, we want to establish a mathematical model to study the combined effects of ROS and CTL immune response on HIV dynamics. To simplify the model analysis, our model only considers the role of oxidative stress in promoting viral infection and ignores the impairment of immune response. We leave that for further investigation.

The rest of the paper is organized as follows. In the next section, reproduction numbers and the existence of possible equilibria are derived. In Sec. 3 we prove the local and global asymptotic stability of the equilibria. In Sec. 4 we perform numerical simulations to illustrate the results derived analytically (such as bistability and periodic solutions) and also explore the role of ROS and CTL immune response in HIV dynamics. Results and a brief discussion are given in Sec. 5.

Reproduction Numbers and Equilibria

In this section, we will derive the reproduction numbers and classify the equilibria for system (1). It is clear that the system (II) always has the disease-free equilibrium (DFE) $\mathbb{E}_0(\frac{\lambda}{d},0,0,0)$. Using the nextgeneration method [Van den Driessche & Watmough, 2002, the matrices for the new infection and the transfer, \mathbb{F} and \mathbb{V} , are given by

$$\mathbb{F} = \begin{pmatrix} 0 & (1-\varepsilon)b_0 \frac{\lambda}{d} \\ 0 & 0 \end{pmatrix}, \quad \mathbb{V} = \begin{pmatrix} d_E + \alpha + \pi & 0 \\ -\pi & \delta \end{pmatrix}.$$

The basic reproduction number can be derived by

$$R_0 = \rho(\mathbb{FV}^{-1}) = \frac{(1 - \varepsilon)b_0\lambda\pi}{d\delta(d_E + \alpha + \pi)},$$

where $\rho(\mathbb{FV}^{-1})$ is the spectral radius of the nonnegative matrix \mathbb{FV}^{-1} . Note that the basic reproduction number R_0 does not involve the effect of ROS. This is because R_0 is obtained by linearizing system \square at DFE $\mathbb{E}_0(\frac{\lambda}{d},0,0,0)$ and using the next generation matrix method. In our model, we hypothesized that ROS indirectly affects the infection rate $\beta(I)$ through the productively infected cells I. At the DFE, there are no productively infected cells (I=0), which leads to the fact that the ROS parameter does not appear in R_0 .

We investigate the existence of equilibria besides the DFE \mathbb{E}_0 . Any equilibrium of system (1)must satisfy the following equations:

$$\begin{cases} \lambda - dT - (1 - \varepsilon)\beta(I)TI + \alpha E = 0, \\ (1 - \varepsilon)\beta(I)TI - (d_E + \alpha + \pi)E = 0, \\ \pi E - \delta I - pIZ = 0, \\ cIZ - bZ = 0. \end{cases}$$
(3)

We calculate the boundary equilibria besides the DFE \mathbb{E}_0 . The boundary (CTL-free) equilibria are located in the hyperplane Z=0. Setting Z=0, it follows from the third equation in (3) that

$$E = -\frac{\delta}{\pi}I. \tag{4}$$

Substituting (4) into the second equation in (3) yields

$$T = \frac{(d_E + \alpha + \pi)\delta}{(1 - \varepsilon)\beta(I)\pi}.$$
 (5)

Substituting (4) and (5) into the first equation in (3), we obtain

$$G(I) = A_1 I^2 + A_2 I + A_3 = 0, (6)$$

where

$$A_1 = (1 - \varepsilon)b_1(d_E + \pi)\delta,$$

$$A_2 = (1 - \varepsilon)[b_0b_2\delta(d_E + \pi) - \lambda\pi b_1]$$

$$+ (d_E + \pi + \alpha)\delta d,$$

$$A_3 = (d_E + \pi + \alpha)\delta db_2(1 - R_0).$$

If any CTL-free equilibria exist, the I variable is the positive root of the quadratic equation G(I) = 0. Let $\Delta = A_2^2 - 4A_1A_3$. We consider two cases:

Case 1. $R_0 > 1$. Equation (6) has a unique solution I_c . This implies that system \square has a unique CTL-free equilibrium, denoted by

$$\mathbb{E}_c = (T_c, E_c, I_c, 0),$$

where

$$T_c = \frac{(d_E + \alpha + \pi)\delta}{(1 - \varepsilon)\beta(I_c)\pi}, \quad E_c = \frac{\delta}{\pi}I_c,$$

$$I_c = \frac{-A_2 + \sqrt{\Delta}}{2A_1}.$$

Case 2. $R_0 < 1$. In this case, Eq. (6) admits two positive solutions I_1 and I_2 [i.e. system \square has two CTL-free equilibria] if $\Delta > 0$ and $A_2 < 0$. Let $\mathbb{E}_1 = (T_1, E_1, I_1, 0)$ and $\mathbb{E}_2 = (T_2, E_2, I_2, 0)$ denote two CTL-free equilibria with

$$T_{1} = \frac{(d_{E} + \alpha + \pi)\delta}{(1 - \varepsilon)\beta(I_{1})\pi}, \quad E_{1} = \frac{\delta}{\pi}I_{1},$$

$$I_{1} = \frac{-A_{2} - \sqrt{\Delta}}{2A_{1}};$$

$$T_{2} = \frac{(d_{E} + \alpha + \pi)\delta}{(1 - \varepsilon)\beta(I_{2})\pi}, \quad E_{2} = \frac{\delta}{\pi}I_{2},$$

$$I_{2} = \frac{-A_{2} + \sqrt{\Delta}}{2A_{1}}.$$

These two solutions coincide when $\Delta = 0$ and $A_2 < 0$. For all other values of Δ or A_2 , there is no positive solution for Eq. (6).

In addition to R_0 , we define the CTL immune response reproduction number of system Van den Driessche & Watmough, 2002; Jiang & Wang, 2014:

$$R_c = \frac{c}{b}I_c,$$

where $\frac{1}{b}$ denotes the average life expectancy of the CTL, and I_c are productively infected cells at \mathbb{E}_c . Hence, R_c represents the average number of CTL activated by productively infected cells when $R_0 >$ 1. Similar to R_c , we define two other CTL immune response reproduction numbers when $R_0 < 1$:

$$R_1 = \frac{c}{b}I_1, \quad R_2 = \frac{c}{b}I_2,$$

where I_1 and I_2 are productively infected cells at \mathbb{E}_1 and \mathbb{E}_2 , respectively.

In the following, we consider the positive equilibrium of model (1), denoted by $\mathbb{E}^* = (T^*, E^*,$ I^*, Z^*). Let $Z \neq 0$. It follows from the fourth equation in (3) that

$$I^* = \frac{b}{c}. (7)$$

Substituting (7) into the first to third equations of Eq. (3), and after some algebraic manipulations, we obtain

2150203

$$T^* = \frac{\lambda}{d} - \frac{d_E + \pi}{d} E^*,$$

$$Z^* = \frac{c\pi}{pb} E^* - \frac{\delta}{p}$$
(8)

and

$$F(E^*) = \lambda - \left(\frac{d(d_E + \alpha + \pi)}{(1 - \varepsilon)\beta(I^*)I^*} + d_E + \pi\right)E^*$$

$$= 0.$$
(9)

From (\mathfrak{Q}) , we have $E^* < \frac{\lambda}{d_E + \pi}$ and $F'(E^*) < 0$. It follows from the expression of Z^* that the existence of the positive equilibrium \mathbb{E}^* is equivalent to $E^* \in (\frac{b\delta}{c\pi}, \frac{\lambda}{d_E + \pi})$. Noticing $F(\frac{\lambda}{d_E + \pi}) < 0$, we know that the existence of the positive equilibrium \mathbb{E}^* is equivalent to $F(\frac{b\delta}{c\pi}) > 0$. We also consider two cases:

Case 1. $R_0 > 1$. If $R_c < 1$, then $E_c < \frac{b\delta}{c\pi}$ and

$$F\left(\frac{b\delta}{c\pi}\right) = \lambda - \frac{d(d_E + \alpha + \pi)}{(1 - \varepsilon)\beta(I^*)I^*} \frac{b\delta}{c\pi} - (d_E + \pi) \frac{b\delta}{c\pi},$$

$$< \lambda - \frac{d(d_E + \alpha + \pi)}{(1 - \varepsilon)\beta(I_c)\frac{\pi}{\delta}} - (d_E + \pi)E_c$$

$$= 0,$$
(10)

which means $F(\frac{b\delta}{c\pi}) < 0$ if $R_c < 1$. Then there is no equilibrium when $R_c < 1$. If $R_c > 1$, then $E_c > \frac{b\delta}{c\pi}$ and $F(\frac{b\delta}{c\pi}) > 0$. Therefore, there exists a positive equilibrium $\mathbb{E}^* = (T^*, E^*, I^*, Z^*)$ when $R_0 > 1$ and $R_c > 1$.

Case 2. $R_0 < 1$. In this case, it is challenging to analytically determine the existence condition for the positive equilibrium of system (II). Thus, we illustrate it by numerical investigations using different parameter values (Fig. 3).

We summarize the above results in the following theorem.

Theorem 1. For the system of ODEs (1)

(a) The DFE $\mathbb{E}_0 = (\frac{\lambda}{d}, 0, 0, 0)$ always exists.

(b) If $R_0 > 1$, there exists a unique CTL-free equilibrium

$$\mathbb{E}_c = \left(\frac{(d_E + \alpha + \pi)\delta}{(1 - \varepsilon)\beta \left(\frac{-A_2 + \sqrt{\Delta}}{2A_1}\right)\pi}, \frac{\delta}{\pi} \frac{-A_2 + \sqrt{\Delta}}{2A_1}, \frac{-A_2 + \sqrt{\Delta}}{2A_1}, 0\right).$$

(c) If $R_0 < 1$, then system (1) has two CTL-free equilibria

$$\mathbb{E}_{1} = \left(\frac{(d_{E} + \alpha + \pi)\delta}{(1 - \varepsilon)\beta \left(\frac{-A_{2} - \sqrt{\Delta}}{2A_{1}}\right)\pi}, \frac{\delta}{2A_{1}}, \frac{-A_{2} - \sqrt{\Delta}}{2A_{1}}, \frac{-A_{2} - \sqrt{\Delta}}{2A_{1}}, 0\right)$$

and

$$\mathbb{E}_2 = \left(\frac{(d_E + \alpha + \pi)\delta}{(1 - \varepsilon)\beta \left(\frac{-A_2 + \sqrt{\Delta}}{2A_1}\right)\pi}, \frac{\delta}{\pi} \frac{-A_2 + \sqrt{\Delta}}{2A_1}, \frac{-A_2 + \sqrt{\Delta}}{2A_1}, 0\right)$$

if $\Delta > 0$ and $A_2 < 0$. These two equilibria coincide when $\Delta = 0$ and $A_2 < 0$. In other cases, there is no positive CTL-free equilibrium.

(d) If $R_0 > 1$ and $R_c > 1$, the system (\square) has a positive equilibrium of the form $\mathbb{E}^* = (T^*, E^*, I^*, Z^*)$ with $E^* \in (\frac{b\delta}{c\pi}, \frac{\lambda}{d_E + \pi}), T^* = \frac{\lambda}{d} - \frac{d_E + \pi}{d} E^*, I^* = \frac{b}{c}, \text{ and } Z^* = \frac{c\pi}{pb} E^* - \frac{\delta}{p}.$

3. Stability Analysis

In this section, we study the local and global stabilities of equilibria $\mathbb{E}_0, \mathbb{E}_c, \mathbb{E}_1$ and \mathbb{E}_2 .

3.1. Local stability of DFE \mathbb{E}_0

Theorem 2. The DFE \mathbb{E}_0 is locally asymptotically stable (L.A.S) if $R_0 < 1$, and unstable if $R_0 > 1$.

Proof. The Jacobian matrix at \mathbb{E}_0 has two negative eigenvalues -d, -b, and the other two roots are determined by the following matrix

$$Q = \begin{pmatrix} -(d_E + \alpha + \pi) & -(1 - \varepsilon)b_0\lambda\pi \\ -\pi & -\delta \end{pmatrix}.$$
 (11)

It is easy to check that all eigenvalues of Q are negative if and only if $R_0 < 1$, i.e. \mathbb{E}_0 is L.A.S if $R_0 < 1$ and unstable if $R_0 > 1$.

3.2. Local stability of CTL-free equilibria \mathbb{E}_c , \mathbb{E}_1 and \mathbb{E}_2

Let $\hat{\mathbb{E}} = (\hat{T}, \hat{E}, \hat{I}, 0)$ represent any CTL-free equilibrium of system \blacksquare . Then the characteristic equation at $\hat{\mathbb{E}}$ can be expressed as

$$\begin{vmatrix} -d - (1 - \varepsilon)\beta(\hat{I}) - \xi & \alpha & -(1 - \varepsilon)\beta'(\hat{I})\hat{T}\hat{I} - (1 - \varepsilon)\beta(\hat{I})\hat{T} & 0\\ (1 - \varepsilon)\beta(\hat{I}) & -(d_E + \alpha + \pi) - \xi & (1 - \varepsilon)\beta'(\hat{I})\hat{T}\hat{I} + (1 - \varepsilon)\beta(\hat{I})\hat{T} & 0\\ 0 & \pi & -\delta - \xi & -p\hat{I}\\ 0 & 0 & c\hat{I} - b - \xi \end{vmatrix} = 0, \quad (12)$$

where ξ denotes the eigenvalue. Equation (12) can be simplified to

$$(c\hat{I} - b - \xi)(\xi^3 + a_1\xi^2 + a_2\xi + a_3) = 0, \quad (13)$$

where

$$a_1 = d + (1 - \varepsilon)\beta(\hat{I})\hat{I} + d_E + \pi + \delta + \alpha > 0,$$

$$a_2 = (d + (1 - \varepsilon)\beta(\hat{I})\hat{I})(d_E + \pi + \delta)$$

$$+ (d_E + \pi)\delta + \alpha(d + \delta) - \pi((1 - \varepsilon)\beta'(\hat{I})\hat{T}\hat{I}$$
$$+ (1 - \varepsilon)\beta(\hat{I})\hat{T}),$$
$$a_3 = \frac{\hat{I}}{(b_2 + \hat{I})}(2A_1\hat{I} + A_2),$$

in which A_1 and A_2 are given in (6).

Let $W^s(\hat{\mathbb{E}})$, $W^u(\hat{\mathbb{E}})$ and $W^c(\hat{\mathbb{E}})$ be the stable manifold, unstable manifold and center manifold of E, respectively. We have the following local stability results for the CTL-free equilibria \mathbb{E}_c , \mathbb{E}_1 and \mathbb{E}_2 .

Theorem 3

- (a) Assume that $R_0 > 1$.
- (i) If $R_c < 1$ and H > 0, then $\dim[W^s(\mathbb{E}_c)] =$ 4, i.e. the unique CTL-free equilibrium \mathbb{E}_c is L.A.S.;
- (ii) If $R_c < 1$ and H < 0, then $\dim[W^s(\mathbb{E}_c)] = 2$, $\dim[W^u(\mathbb{E}_c)] = 2$, i.e. the unique CTL-free equilibrium \mathbb{E}_c is unstable;
- (iii) If $R_c < 1$ and H = 0, then $\dim[W^s(\mathbb{E}_c)] = 2$, $\dim[W^c(\mathbb{E}_c)]=2.$
- (b) Assume that $R_0 < 1$ and both \mathbb{E}_1 and \mathbb{E}_2 exist.
- (i) $\dim[W^s(\mathbb{E}_1)] = 3$, $\dim[W^u(\mathbb{E}_1)] = 1$, *i.e.* the CTL-free equilibrium \mathbb{E}_1 is unstable;
- (ii) If $R_2 < 1$ and H > 0, then $\dim[W^s(\mathbb{E}_2)] = 4$, i.e. the CTL-free equilibrium \mathbb{E}_2 is L.A.S.;
- (iii) If $R_2 < 1$ and H < 0, then $\dim[W^s(\mathbb{E}_2)] = 2$, $\dim[W^u(\mathbb{E}_2)] = 2$, i.e. the CTL-free equilibrium \mathbb{E}_2 is unstable;
- (iv) If $R_2 < 1$ and H = 0, then $\dim[W^s(\mathbb{E}_2)] = 2$, $\dim[W^c(\mathbb{E}_2)] = 2.$

Proof. Equation (13) has a solution $\xi_1 = c\hat{I} - b$. Let ξ_2, ξ_3 and ξ_4 be the remaining eigenvalues and we assume that the real part satisfies $\Re(\xi_2)$ < $\Re(\xi_3) < \Re(\xi_4)$.

(1) Assume $R_0 > 1$. The system (1) has a unique CTL-free equilibrium $\mathbb{E}_c = (T_c, E_c, I_c, 0)$, where I_c is a root of (6) and satisfies $G'(I_c) = 2A_1I_c +$ $A_2 > 0$. We know that $\xi_1 = cI_c - b < 0$ is equivalent to $R_c < 1$. The remaining eigenvalues, ξ_2, ξ_3 and ξ_4 , are determined by the following equation

$$\xi^3 + a_1 \xi^2 + a_2 \xi + a_3 = 0, \tag{14}$$

where a_1, a_2, a_3 are defined as above (13). From the relations between roots and coefficients, it can be obtained that

$$\xi_2 + \xi_3 + \xi_4 = -a_1 < 0,$$

$$\xi_2 \xi_3 \xi_4 = -a_3 = -\frac{I_c}{(b_2 + I_c)} (2A_1 I_c + A_2) < 0.$$

This means either $\Re(\xi_2) < \Re(\xi_3) < \Re(\xi_4) < 0$ or $\Re(\xi_2) < 0 < \Re(\xi_3) < \Re(\xi_4)$. Thus, the stability of \mathbb{E}_c completely depends on the sign of $a_1a_2 - a_3$. For simplicity, let $H = a_1 a_2 - a_3$.

If H > 0, then the Routh-Hurwitz criterion implies that $\Re(\xi_2) < \Re(\xi_3) < \Re(\xi_4) < 0$. By the center manifold theorem, we have $\dim[W^s(\mathbb{E}_c)] = 4$, i.e. the unique CTL-free equilibrium \mathbb{E}_c is L.A.S. If H = 0, then substituting $a_1a_2 = a_3$ into the left-hand side of Equ. (14) yields two roots $\pm \sqrt{a_2}i$, which means $\Re(\xi_2) < 0$. By the center manifold theorem, we have $\dim[W^s(\mathbb{E}_c)] = 2$, $\dim[W^c(\mathbb{E}_c)] = 2$. If H < 0, then the Routh–Hurwitz criterion implies that $\Re(\xi_2) < 0 < \Re(\xi_3) < \Re(\xi_4)$. By the center manifold theorem, we have $\dim[W^s(\mathbb{E}_c)] = 2$, $\dim[W^u(\mathbb{E}_c)] = 2$, i.e. the unique CTL-free equilibrium \mathbb{E}_c is unstable.

 $I_1,0)$ and $\mathbb{E}_2=(T_2,E_2,I_2,0)$ exist, where I_1 and I_2 are the roots of Eq. (6). Furthermore, I_1 and I_2 satisfy

$$G'(I_1) = 2A_1I_1 + A_2 < 0,$$

$$G'(I_2) = 2A_1I_2 + A_2 > 0,$$

respectively. Similarly, we can obtain the stability of \mathbb{E}_2 by using the same analysis method as \mathbb{E}_c . Therefore, we focus on the stability of \mathbb{E}_1 . It is clear that $\xi_1 = cI_1 - b < 0$ is equivalent to $R_1 < 1$. It follows from the relations between roots and coefficients that

$$\xi_2 + \xi_3 + \xi_4 = -a_1 < 0,$$

$$\xi_2 \xi_3 \xi_4 = -a_3 = -\frac{I_1}{(b_2 + I_1)} (2A_1 I_1 + A_2) > 0.$$

This means $\Re(\xi_2) < 0$, and $\Re(\xi_3)$ and $\Re(\xi_4)$ have different signs. Thus, we have

$$\dim[W^s(\mathbb{E}_1)] = 3, \quad \dim[W^u(\mathbb{E}_1)] = 1,$$

that is, \mathbb{E}_1 is a saddle point. This completes the proof of Theorem 3

3.3. Global stability of the CTL-free equilibrium \mathbb{E}_c

For the equilibrium \mathbb{E}_c to be feasible, we always assume that $R_0 > 1$ in this subsection. In the following, we examine the global stability of the CTL-free equilibrium \mathbb{E}_c .

Theorem 4. The CTL-free equilibrium \mathbb{E}_c of system \square is globally asymptotically stable if $R_c < 1 <$ R_0 and $dT_c - \alpha E_c > 0$.

Q. Deng et al.

Proof. Define

$$V(T, E, I, Z) = T - T_c - \int_{T_c}^{T} \frac{H_c(b_2 + I_c)}{(1 - \varepsilon)(b_0 b_2 + b_1 I_c) I_c s} ds + \frac{\alpha}{2(d + d_E + \pi) T_c} (T - T_c + E - E_c)^2 + \frac{H_c}{\pi E_c} \left(I - I_c - I_c \ln \frac{I}{I_c} \right) + E - E_c - E_c \ln \frac{E}{E_c} + \frac{pH_c}{c\pi E_c} Z,$$

$$(15)$$

where

$$H_c = (1 - \varepsilon) \frac{b_0 b_2 + b_1 I_c}{b_2 + I_c} I_c T_c.$$

Calculating the derivative of V(T, E, I, Z)along the positive solutions of system (1), we obtain

$$\frac{dV}{dt}\Big|_{(1)} = \left(1 - \frac{H_c(b_2 + I_c)}{(1 - \varepsilon)(b_0 b_2 + b_1 I_c) I_c T}\right) \frac{dT}{dt} + \frac{\alpha}{(d + d_E + \pi) T_c} (T - T_c + E - E_c) \times \left(\frac{dT}{dt} + \frac{dE}{dt}\right) + \frac{H_c}{\pi E_c} \left(1 - \frac{I_c}{I}\right) \frac{dI}{dt} + \left(1 - \frac{E_c}{E}\right) \frac{dE}{dt} + \frac{pH_c}{c\pi E_c} \frac{dZ}{dt}. \tag{16}$$

Noting that

$$\lambda = dT_c + H_c - \alpha E_c, \quad \pi E_c = \delta I_c,$$
$$H_c = (d_E + \alpha + \pi) E_c$$

and

$$\frac{T - T_c}{T} = -\frac{(T - T_c)^2}{TT_c} + \frac{T - T_c}{T_c},$$

$$\begin{aligned} \frac{\mathrm{d}V}{\mathrm{d}t}\Big|_{(1)} &= \left(1 - \frac{T_c}{T}\right) (dT_c + H_c - \alpha E_c - dT - (1 - \varepsilon)\beta(I)IT + \alpha E) \\ &+ \frac{\alpha}{(d + d_E + \pi)T_c} (T - T_c + E - E_c) (dT_c + H_c - \alpha E_c - dT + \alpha E - (d_E + \alpha + \pi)E) \\ &+ \frac{H_c}{\pi E_c} \left(1 - \frac{I_c}{I}\right) (\pi E - \delta I - pIZ) + \left(1 - \frac{E_c}{E}\right) ((1 - \varepsilon)\beta(I)IT - (d_E + \alpha + \pi)E) \\ &+ \frac{pH_c}{c\pi E_c} (cIZ - bZ) \\ &= \frac{-d(T - T_c)^2}{T} + \frac{\alpha(E - E_c)(T - T_c)}{T} + H_c - \frac{H_c^2(b_2 + I_c)}{(1 - \varepsilon)(b_0b_2 + b_1I_c)I_cT} + \frac{H_cI(b_0b_2 + b_1I)(b_2 + I_c)}{I_c(b_0b_2 + b_1I_c)(b_2 + I)} \\ &+ \frac{H_c(b_0b_2 + b_1I_c)(b_2 + I)}{(b_0b_2 + b_1I)(b_2 + I_c)} - \frac{H_c(b_0b_2 + b_1I_c)(b_2 + I)}{(b_0b_2 + b_1I)(b_2 + I_c)} + \frac{\alpha(E - E_c)(T_c - T)}{T_c} - \frac{\alpha d(T - T_c)^2}{(d_E + \pi + d)T_c} \\ &- \frac{\alpha(d_E + \pi)(E - E_c)^2}{(d_E + \pi + d)T_c} - \frac{H_1\delta I}{\pi E_c} - \frac{I_cH_cE}{E_cI} + \frac{H_cI_c\delta}{\pi E_c} + \frac{H_cI_cpZ}{\pi E_c} - (1 - \varepsilon)\frac{E_c}{E}\frac{b_0b_2 + b_1I}{b_2 + I}IT \\ &+ (d_E + \alpha + \pi)E_c - \frac{pH_c}{c\pi E_c}bZ \end{aligned}$$

$$= -\left(dT_c - \alpha E_c + \alpha E + \frac{\alpha dT}{d_E + \pi + d}\right) \frac{(T - T_c)^2}{TT_c} - \frac{\alpha(d_E + \pi)(E - E_c)^2}{(d_E + \pi + d)T_c} + \frac{bH_cp}{c\pi E_c}(R_c - 1)Z \right.$$

$$- \frac{H_c(b_1b_2 - b_0b_2)(b_1I_cI + b_0b_2^2 + b_1b_2)(I - I_c)^2}{(b_0b_2 + b_1I_c)(b_2 + I_c)(b_0b_2 + b_1I)(b_2 + I_c)}$$

$$+ H_c\left(4 - \frac{T_c}{T} - \frac{EI_c}{E_cI} - \frac{(b_2 + I_c)(b_0b_2 + b_1I)ITE_c}{(b_0 + I_c)(b_0b_2 + b_1I)(b_2 + I_c)}\right). \tag{17}$$

Effect of Reactive Oxygen Species and CTL Immune Response on HIV Dynamics

According to Inequality of arithmetic and geometric means (the arithmetic mean is greater than or equal to the geometric mean, i.e. $\frac{x_1+x_2+\cdots+x_n}{n} \geq \sqrt[n]{x_1x_2\cdots x_n}$), it follows that

$$\frac{1}{4} \left(\frac{T_c}{T} + \frac{EI_c}{E_c I} + \frac{(b_2 + I_c)(b_0 b_2 + b_1 I)ITE_c}{(b_2 + I)(b_0 b_2 + b_1 I_c)I_c T_c E} + \frac{(b_0 b_2 + b_1 I_c)(b_2 + I)}{(b_0 b_2 + b_1 I)(b_2 + I_c)} \right)$$

$$\geq \sqrt[4]{\frac{T_c}{T} \times \frac{EI_c}{E_c I}} \times \frac{(b_2 + I_c)(b_0 b_2 + b_1 I)ITE_c}{(b_2 + I)(b_0 b_2 + b_1 I_c)I_c T_c E} \times \frac{(b_0 b_2 + b_1 I_c)(b_2 + I)}{(b_0 b_2 + b_1 I)(b_2 + I_c)} = 1.$$

Then

$$4 - \frac{T_c}{T} - \frac{EI_c}{E_cI} - \frac{(b_2 + I_c)(b_0b_2 + b_1I)ITE_c}{(b_2 + I)(b_0b_2 + b_1I_c)I_cT_cE} - \frac{(b_0b_2 + b_1I_c)(b_2 + I)}{(b_0b_2 + b_1I)(b_2 + I_c)} \le 0.$$

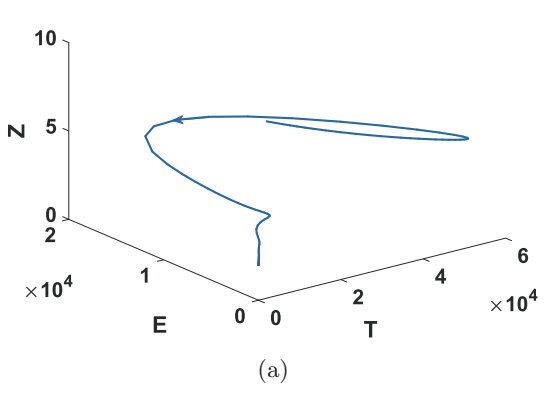
Hence, when $R_c < 1$ and $dT_c - \alpha E_c > 0$, the inequality $\frac{\mathrm{d}V}{\mathrm{d}t}|_{(1)} \leq 0$ holds. We note that $\frac{\mathrm{d}V}{\mathrm{d}t}|_{(1)} = 0$ if and only if $T = T_c$, $E = E_c$ and $I = I_c$ for all t. Thus, by LaSalle's invariance principle, the CTL-free equilibrium \mathbb{E}_c is globally asymptotically stable.

4. Numerical Results

In this section, we perform numerical simulations to further investigate the dynamical behavior of the model solutions and also explore the effect of ROS and CTL immune response on HIV dynamics. Most of the parameter values are chosen from experimental data and modeling literature Rong et al., 2007c; Perelson et al., 1993; Rong et al., 2007a; Shiri et al., 2005; Wodarz & Lloyd, 2004; Wang et al., 2012]. Because ROS can promote viral infection, we assume that the maximum infection rate may be 100 times higher than that in the absence of ROS. The infection rate in the absence of ROS (b₀) is

assumed to be in the interval $(2.5 \times 10^{-8} \text{ mL day}^{-1}, 5 \times 10^{-4} \text{ mL day}^{-1})$ [Wang et al.], [2009]. Thus, the maximum infection rate (b_1) is in the interval $(2.5 \times 10^{-6} \text{ mL day}^{-1}, 5 \times 10^{-2} \text{ mL day}^{-1})$. The constant b_2 is assumed to be in the interval $(0.0001 \text{ mL}^{-1}, 0.1 \text{ mL}^{-1})$. All parameter values used are summarized in Table [1]

In Figs. 2 and 3, we aim to show the dynamics behavior of the system when $R_0 > 1$ and $R_0 < 1$, respectively. Thus, the parameter values used in the simulations are chosen for illustration purposes. The parameter values also have biological meaning as most of them are from experimental data and modeling literature. Figure 2 shows the dynamics of the solutions of system (1) when $R_0 > 1$. In Fig. 2(a), the parameters in Table 1 are used and $\varepsilon = 0.6$, $b_0 = 2.4 \times 10^{-5}$, $b_1 = 3 \times 10^{-4}$, $b_2 = 0.001$, c = 0.00001. With these parameter values, we have $R_0 = 5.8343 > 1$, $R_c = 0.6034 < 1$, H = 9.9918 > 0 and $dT_c - \alpha E_c = 72.3319 > 0$.



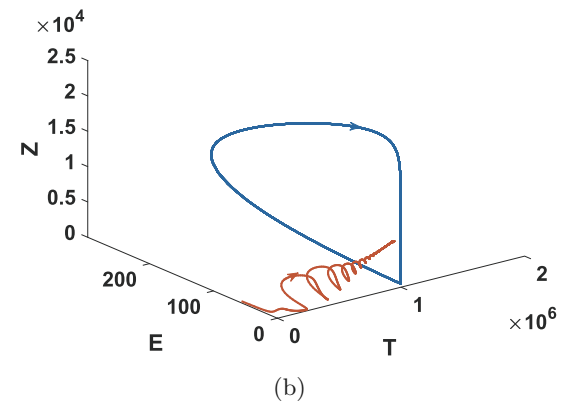


Fig. 2. Dynamics of the solutions of system (II) when $R_0 > 1$. (a) Solution trajectories of the system converge to the CTL-free equilibrium \mathbb{E}_c when $R_c < 1$. The parameters given in Table II are used and $\varepsilon = 0.6$, $b_0 = 2.4 \times 10^{-5}$, $b_1 = 3 \times 10^{-4}$, $b_2 = 0.001$, c = 0.00001. In this case, $R_0 = 5.8343 > 1$, $R_c = 0.6034 < 1$, H = 9.9918 > 0 and $dT_c - \alpha E_c = 72.3319 > 0$ and (b) emergence of bistability. It shows that solutions will converge to either the positive equilibrium \mathbb{E}^* (red orbit) or the stable limit cycle (blue orbit) depending on initial conditions when $R_c > 1$. The parameters given in Table II are used and $\varepsilon = 0.6$, $b_0 = 2.4 \times 10^{-5}$, $b_1 = 3 \times 10^{-5}$, $b_2 = 0.001$, c = 0.1. In this case, $R_0 = 5.8343 > 1$ and $R_c = 5.6456 \times 10^3 > 1$.

Q. Deng et al.

In this case, all the solutions converge to the CTL-free equilibrium \mathbb{E}_c . This agrees with Theorem \mathbb{E}_c of Part 3. With the parameter values used in Fig. $\mathbb{Z}(b)$ (the same as (a) expect $b_1 = 3 \times 10^{-5}$, c = 0.1), the basic reproduction number is $R_0 = 5.8343 > 1$ and the CTL immune response reproduction number is $R_c = 5.6456 \times 10^3 > 1$. In this case, we see the occurrence of bistability, where a stable positive equilibrium coexists with a stable limit cycle. Specifically, solutions starting from near \mathbb{E}^* will converge to \mathbb{E}^* , while solutions with initial conditions not close to \mathbb{E}^* will converge to a stable periodic solution [Fig. $\mathbb{Z}(b)$]. The solutions in Fig. $\mathbb{Z}(a)$ converge to the CTL-free equilibrium \mathbb{E}_c , implying that the

HIV infection becomes chronic but CTL immune response is absent in such a situation. While in Fig. $\square(b)$, the bistability of positive equilibrium and limit cycle means that both CTL immune response and viral infection have been successfully established in this case. This is because we assume that the generation rate of CTL in Fig. $\square(b)$ (c = 0.1) is much stronger than that in Fig. $\square(a)$ (c = 0.00001).

In Fig. 3 with the chosen parameters we have $R_0 < 1$. We chose b_1 and c as bifurcation parameters to simulate the dynamics of the solutions for system (1). The values are $(b_1, c) = (10^{-6}, 0.00003)$, $(b_1, c) = (3 \times 10^{-6}, 0.00003)$, $(b_1, c) = (3 \times 10^{-4}, 0.0003)$ and $(b_1, c) = (3 \times 10^{-6}, 0.0003)$ in

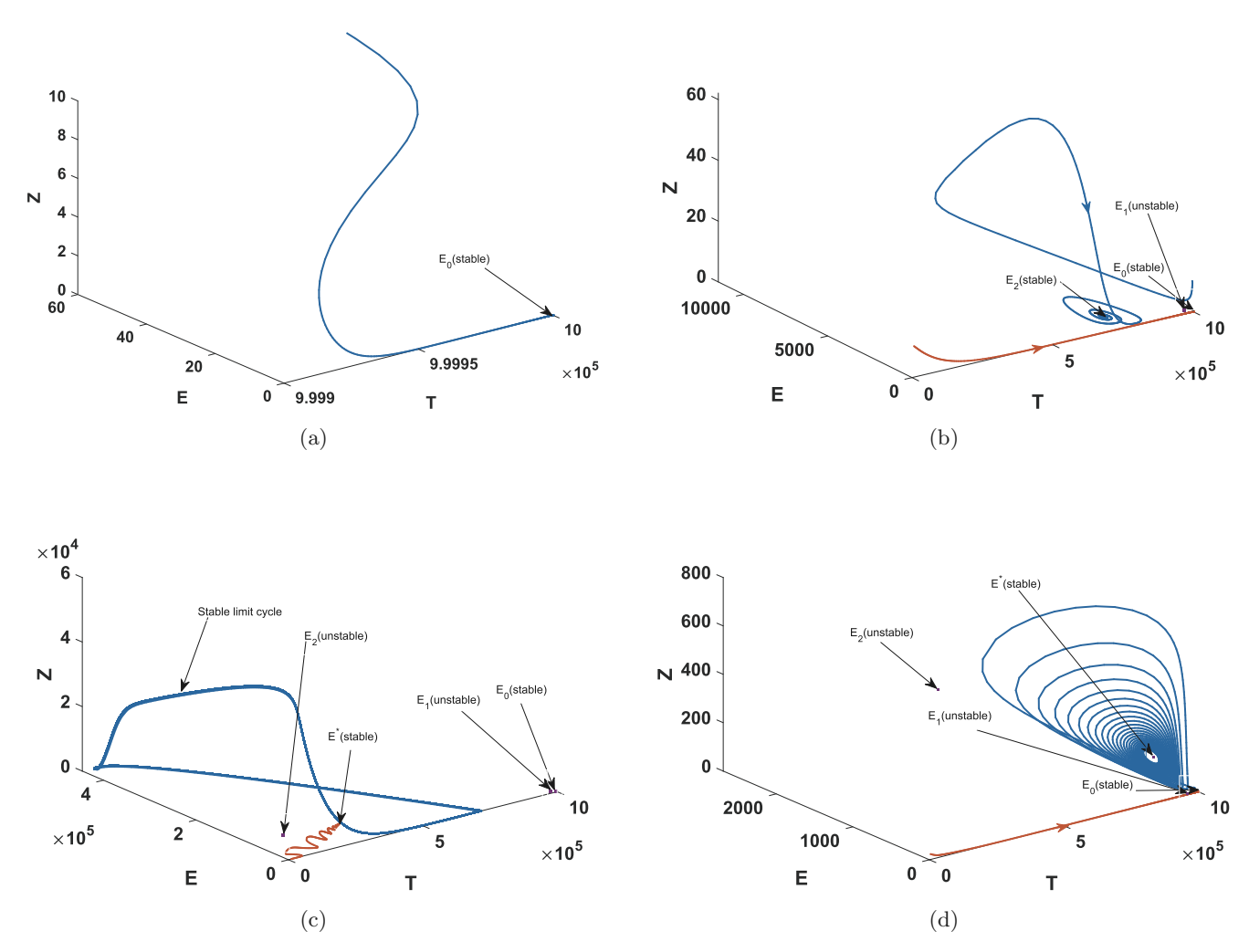


Fig. 3. Dynamics of the solutions of system (II) when $R_0 < 1$. Parameters from Table II are used and $\varepsilon = 0.6$, $b_0 = 2.4 \times 10^{-6}$, $b_2 = 0.0001$. The parameters b_1 and c are chosen as bifurcation parameters. (a) For $b_1 = 10^{-6}$ and c = 0.00003, solutions will converge to the DFE \mathbb{E}_0 , (b) for $b_1 = 3 \times 10^{-6}$ and c = 0.00003, we have $R_2 = 0.4367 < 1$, H = 5.1806 > 0. Depending on initial conditions, solutions will converge to either the CTL-free equilibrium \mathbb{E}_2 or the DFE \mathbb{E}_0 , (c) for $b_1 = 3 \times 10^{-4}$ and c = 0.0003, we obtain $R_2 = 18.0839$. Solutions will converge to either a stable periodic solution, the positive equilibrium \mathbb{E}^* , or the DFE \mathbb{E}_0 depending on initial conditions and (d) for $b_1 = 3 \times 10^{-6}$ and c = 0.0003, we have $R_2 = 4.3673$. Solutions converge to either the stable positive equilibrium \mathbb{E}^* or the DFE \mathbb{E}_0 , depending on initial conditions.

Figs. 3(a)-3(d), respectively. All other parameter values are listed in Table \blacksquare and $\varepsilon = 0.6$, $b_0 = 2.4 \times 10^{-6}, b_2 = 0.0001$. Figure 3(a) shows that the unique DFE \mathbb{E}_0 is L.A.S when $(b_1, c) =$ $(10^{-6}, 0.00003).$

Figures 3(b)-3(d) shows the emergence of bistable phenomena, which are different from Fig. 3(a). In Fig. 3(b), $(b_1, c) = (3 \times 10^{-6}, 0.00003)$. This leads to $R_2 = 0.4367 < 1$ and H = 5.1806 > 0. The solutions converge to either the CTL-free equilibrium \mathbb{E}_2 or the DFE \mathbb{E}_0 , depending on the initial condition. With $(b_1, c) = (3 \times 10^{-4}, 0.0003)$, $R_2 = 18.0839 > 1$, Fig. (c) displays the phase portraits which show the convergence of the solutions to either a stable periodic solution, the positive equilibrium \mathbb{E}^* , or the DFE \mathbb{E}_0 , depending

on the initial condition. In Fig. 3(d), the choice of parameter values $(b_1, c) = (3 \times 10^{-6}, 0.0003)$ leads to $R_2 = 4.3673$. The blue orbit illustrates the disappearance of the stable limit cycle and the convergence of the solution to the stable positive equilibrium \mathbb{E}^* . The red orbit, whose initial value is located in the basin of attraction for the DFE, converges to the DFE \mathbb{E}_0 . It is worth mentioning that a Hopf bifurcation is only possible from \mathbb{E}_2 . In addition, \mathbb{E}_1 is quite close to \mathbb{E}_0 when it exists. Specifically, $\mathbb{E}_1 = (10^6, 1.2111 \times 10^{-4}, 1.3322 \times 10^{-4}, 0)$ in Figs. 3(b) and 3(d), and $\mathbb{E}_1 = (10^6, 5.2227 \times 10^{-7}, 0)$ 10^{-7} , 5.7449×10⁻⁷, 0) in Fig. 3(c). This may explain the HIV persistence during treatment. We perform the following simulations to further study the factors underlying this phenomenon.

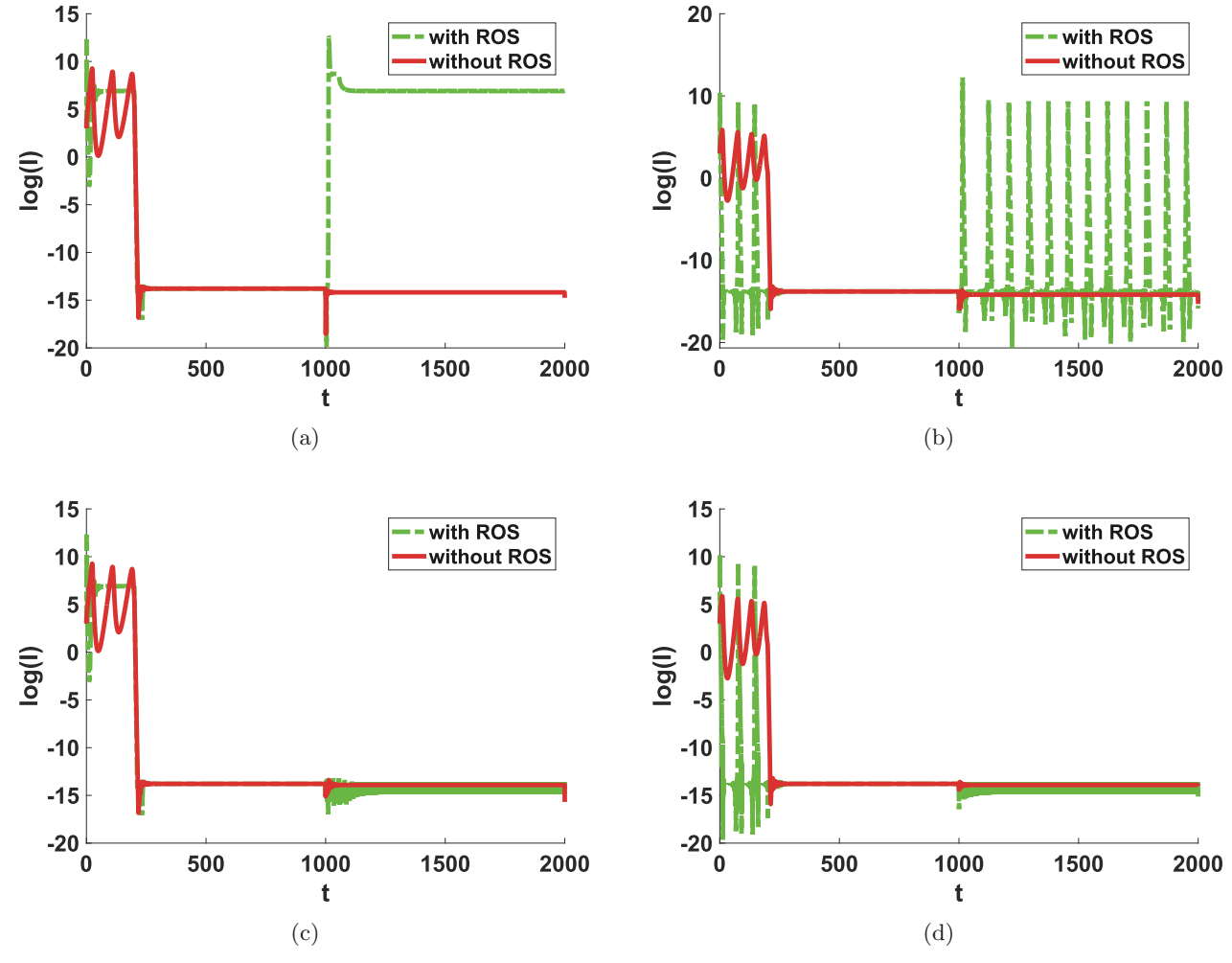


Fig. 4. Dynamics of productively infected cells predicted by the model in different scenarios. The green line is in the presence of ROS $(b_1 = 3 \times 10^{-4})$, while the red line is without ROS $(b_1 = b_0)$. The initial drug efficacy is 100% during the period 200 to 1000 days and then reduces on t=1000 days. In (a) and (b), the drug efficacy decreases to 0.5 at t=1000, and in (a) the parameter values are chosen from Table \blacksquare and $b_0=2.4\times 10^{-6},\ b_2=0.0001,\ c=0.0001$. In (b), the parameter values are the same as those in (a) except c = 0.003. In (c) and (d), the drug efficacy decreases to 0.75 at t = 1000 and in (c) the parameter values are the same as those in (a). In (d) the parameter values are the same as those in (a) except c = 0.003.

Q. Deng et al.

The dynamics of productively infected cells during treatment are shown in Fig. 4. When t =200 days, the treatment is started and the drug efficacy is reduced when $t = 1000 \,\mathrm{days}$. The green dashed line represents the dynamics in the presence of ROS, while the red solid line represents that without ROS. In Fig. 4(a) and 4(b), the drug treatment is assumed to be 100% effective during the period 200 to 1000 days and after that the drug efficacy is reduced to 0.5 due to certain factors (e.g. drugresistant mutation or drug adherence). We observe from the green dashed line in Fig. 4(a) that productively infected cells are largely inhibited during the initial treatment. When the drug efficacy decreases, the number of productively infected cells immediately increases and then slightly decreases to the equilibrium level. From the red solid line, we find that productively infected cells are expected to remain suppressed for the whole duration of treatment. This indicates that ROS contributes to HIV infection. In order to show the role of CTL immune response, we choose the generation rate of CTL(c) in Fig. 4(b) (c = 0.003) is higher than that in Fig. $\underline{4}$ (a) (c = 0.0001). In the absence of ROS [red solid line in Fig. 4(b), the dynamics of productively infected cells are similar to that in Fig. 4(a), but in the presence of ROS [green dashed line in Fig. 4(b)], the enhanced CTL immune response causes sustained oscillations. This indicates the significant role of both CTL immune response and ROS in HIV replication.

In Figs. $\underline{\underline{\mathbf{4}}}(c)$ and $\underline{\underline{\mathbf{4}}}(d)$, we also assume that the drug treatment is 100% effective from 200 to 1000 days but the drug efficacy is reduced to 0.75 after that period. The CTL immune response in Fig. 4(d) is stronger than that in Fig. 4(c). Compared with Fig. 4(a), productively infected cells with and without ROS in Fig. $\underline{4}(c)$ are both inhibited during therapy. These results suggest that to completely suppress HIV replication the drug efficacy should be maintained at a level greater than 0.75 [the dynamics of productively infected cells with the drug efficacy less than 0.75 are similar to that in Fig. $\underline{4}(a)$ and are omitted here]. A study estimated that the overall drug efficacy was as low as 68% for some combination therapies Louie et al., 2003. Thus, HIV continue to persist despite current drug therapy possibly due to the existence of ROS. From Fig. 4(d), we observe that a stronger CTL immune response gives rise to sustained oscillations before treatment (green dashed line), while the dynamics

after treatment are similar to Fig. $\P(c)$ (both red solid and green dashed lines).

5. Results and Discussion

ROS can enhance HIV replication by activating transcription factors such as NF-kB. Several biological studies have shown that ROS have played an essential role in the development of HIV infection [Israel & Gougerot-Pocidalo, 1997; Romero-Alvira & Roche, 1998]. In this paper, we propose a mathematical model to study the effect of ROS and CTL immune response on HIV dynamics.

Our study shows that including the effect of ROS and CTLs in an HIV infection model leads to very rich dynamics. We obtain four reproductive numbers and prove the local or global asymptotic stability for the DFE (\mathbb{E}_0) and CTL-free equilibria (\mathbb{E}_c , \mathbb{E}_1 and \mathbb{E}_2). Actually, the stability of CTL-free equilibria implies that the HIV infection becomes chronic, but the CTL immune response has not been established. We also study the existence of the positive equilibrium (\mathbb{E}^*) when $R_0 > 1$, and provide numerical examples to illustrate the dynamics of system (II). By numerical investigation, we extend our theoretical results by showing various bistable scenarios and sustained oscillations, which indicate the existence of a Hopf bifurcation (Figs. 2 and 3). Additionally, by comparing the green dashed line in Figs. $\underline{4}(a)$ and $\underline{4}(b)$, we observe that ROS and CTLs give rise to the occurrence of sustained oscillations. Interestingly, these oscillations are also found in other delay models with a biologically meaningful parameter space Ciupe et al., 2006; Wang et al., 2009; Wang et al., 2014].

Antiretroviral drug development has largely suppressed viral replication and prevented transmission and progression to AIDS. However, current treatment cannot achieve a cure of infection. Many mathematical models have been developed to investigate the possible factors that may lead to HIV persistence. As shown in Figs. (4(a) and (4(b)), comparing model (11) to the model without ROS, the ROS can cause an increase in the number of infected cells once the drug efficacy is below a certain level. These results suggest that the presence of ROS in HIV patients may be a factor that prevents viral eradication by the current treatment. This solicits more research on the detrimental influence of ROS in HIV infection.

Effect of Reactive Oxygen Species and CTL Immune Response on HIV Dynamics

Acknowledgments

Z. Qiu was supported by the National Natural Science Foundation of China (12071217). Q. Deng was supported by the CSC (202006840122) and the Postgraduate Research and Practice Innovation Program of Jiangsu Province (KYCX21_0250). T. Guo was supported by the Postgraduate Research and Practice Innovation Program of Jiangsu Province (KYCX20_0243). L. Rong was supported by NSF grant DMS-1950254.

References

- Allali, K., Danane, J. & Kuang, Y. [2017] "Global analysis for an HIV infection model with CTL immune response and infected cells in eclipse phase," Appl. Sci. 7, 861.
- Bartholdy, C., Christensen, J. P., Wodarz, D. & Thomsen, A. R. [2000] "Persistent virus infection despite chronic cytotoxic T-lymphocyte activation in gamma interferon-deficient mice infected with lymphocytic choriomeningitis virus," J. Virol. 74, 10304–10311.
- Ciupe, M., Bivort, B., Bortz, D. & Nelson, P. [2006] "Estimating kinetic parameters from HIV primary infection data through the eyes of three different mathematical models," Math. Biosci. 200, 1–27.
- Deng, Q., Qiu, Z., Guo, T. & Rong, L. [2021] "Modeling within-host viral dynamics: The role of CTL immune responses in the evolution of drug resistance," Discr. Contin. Dyn. Syst. B 26, 3543-3562.
- Feng, T. & Qiu, Z. [2019] "Global analysis of a stochastic TB model with vaccination and treatment," Discr. Contin. Dyn. Syst. B 24, 2923–2939.
- Feng, T., Qiu, Z. & Meng, X. [2019] "Dynamics of a stochastic hepatitis c virus system with host immunity," Discr. Contin. Dyn. Syst. B 24, 6367-6385.
- Flores, S. C., Marecki, J. C., Harper, K. P., Bose, S. K., Nelson, S. K. & McCord, J. M. [1993] "Tat protein of human immunodeficiency virus type 1 represses expression of manganese superoxide dismutase in HeLa cells," P. Natl A. Sci. 90, 7632–7636.
- Gil, L., Martínez, G., González, I., Tarinas, A., Álvarez, A., Giuliani, A., Molina, R., Tápanes, R., Pérez, J. & León, O. S. [2003] "Contribution to characterization of oxidative stress in HIV/AIDS patients," Pharmacol. Res. 47, 217–224.
- Gloire, G., Legrand-Poels, S. & Piette, J. [2006] "NF- κ B activation by reactive oxygen species: Fifteen years later," Biochem. Pharmacol. 72, 1493–1505.
- Guo, T. & Qiu, Z. [2019] "The effects of CTL immune response on HIV infection model with potent therapy, latently infected cells and cell-to-cell viral transmission," Math. Biosci. Eng. 16, 6822-6841.

- Guo, T., Qiu, Z. & Rong, L. [2020a] "Modeling the role of macrophages in HIV persistence during antiretroviral therapy," J. Math. Biol. 81, 369-402.
- Guo, T., Qiu, Z. & Rong, L. [2020b] "A within-host drug resistance model with continuous state-dependent viral strains," Appl. Math. Lett. 104, 106223.
- Hildeman, D. A. [2004] "Regulation of T-cell apoptosis by reactive oxygen species," Free Radical Bio. Med. **36**, 1496–1504.
- Israel, N. & Gougerot-Pocidalo, M.-A. [1997] "Oxidative stress in human immunodeficiency virus infection," Cell. Mol. Life Sci. 53, 864-870.
- Jiang, C. & Wang, W. [2014] "Complete classification of global dynamics of a virus model with immune responses," Discr. Contin. Dyn. Syst. B 19, 1087-
- Louie, M., Hogan, C., Di Mascio, M., Hurley, A., Simon, V., Rooney, J., Ruiz, N., Brun, S., Sun, E., Perelson, A. S. et al. [2003] "Determining the relative efficacy of highly active antiretroviral therapy," J. Infect. Dis. **187**, 896–900.
- Lv, C., Huang, L. & Yuan, Z. [2014] "Global stability for an HIV-1 infection model with Beddington-DeAngelis incidence rate and CTL immune response," Commun. Nonlin. Sci. Numer. Simul. 19, 121–127.
- Maziane, M., Hattaf, K. & Yousfi, N. [2017] "Global stability for a class of HIV infection models with cure of infected cells in eclipse stage and CTL immune response," Int. J. Dyn. Control 5, 1035–1045.
- Nowak, M. & May, R. M. [2000] Virus Dynamics: Mathematical Principles of Immunology and Virology: Mathematical Principles of Immunology and Virology (Oxford University Press, UK).
- Pace, G. W. & Leaf, C. D. [1995] "The role of oxidative stress in HIV disease," Free Radical Bio. Med. **19**, 523–528.
- Perelson, A. S., Kirschner, D. E. & De Boer, R. [1993] "Dynamics of HIV infection of CD4+ T cells," Math. Biosci. 114, 81–125.
- Perelson, A. S. & Nelson, P. W. [1999] "Mathematical analysis of HIV-1 dynamics in vivo," SIAM Rev. 41,
- Romero-Alvira, D. & Roche, E. [1998] "The keys of oxidative stress in acquired immune deficiency syndrome apoptosis," Med. Hypotheses 51, 169–173.
- Rong, L., Feng, Z. & Perelson, A. S. [2007a] "Emergence of HIV-1 drug resistance during antiretroviral treatment," Bull. Math. Biol. 69, 2027–2060.
- Rong, L., Feng, Z. & Perelson, A. S. [2007b] "Mathematical analysis of age-structured HIV-1 dynamics with combination antiretroviral therapy," SIAM J. Appl. Math. 67, 731–756.
- Rong, L., Gilchrist, M. A., Feng, Z. & Perelson, A. S. [2007c] "Modeling within-host HIV-1 dynamics and the evolution of drug resistance: Trade-offs between

Q. Deng et al.

- viral enzyme function and drug susceptibility," J. Theor. Biol. 247, 804-818.
- Rong, L. & Perelson, A. S. [2009] "Modeling latently infected cell activation: Viral and latent reservoir persistence, and viral blips in HIV-infected patients on potent therapy," PLoS Comput. Biol. 5, e1000533.
- Schwarz, K. B. [1996] "Oxidative stress during viral infection: A review," Free Radical Bio. Med. 21, 641-649.
- Shiri, T., Garira, W. & Musekwa, S. D. [2005] "A two-strain HIV-1 mathematical model to assess the effects of chemotherapy on disease parameters," Math. Biosci. Eng. 2, 811-832.
- Souza, M. O. & Zubelli, J. P. [2011] "Global stability for a class of virus models with Cytotoxic T Lymphocyte immune response and antigenic variation," Bull. Math. Biol. 73, 609–625.
- Stephensen, C. B., Marquis, G. S., Douglas, S. D. & Wilson, C. M. [2005] "Immune activation and oxidative damage in HIV-positive and HIV-negative adolescents," JAIDS 38, 180-190.
- Sun, C., Hsieh, Y. H. & Georgescu, P. [2018] "A model for HIV transmission with two interacting high-risk groups," Nonlin. Anal.: Real World Appl. 40, 170-184.
- Tang, A. M. & Smit, E. [2000] "Oxidative stress in HIV-1-infected injection drug users," JAIDS 25, S12–S18.
- Van den Driessche, P. & Watmough, J. [2002] "Reproduction numbers and sub-threshold endemic equilibria for compartmental models of disease transmission," Math. Biosci. 180, 29–48.
- van Gaalen, R. D. & Wahl, L. M. [2009] "Reconciling conflicting clinical studies of antioxidant supplementation as HIV therapy: A mathematical approach," BMC Public Health 9, 1–18.

- Wang, Y., Zhou, Y., Wu, J. & Heffernan, J. [2009] "Oscillatory viral dynamics in a delayed HIV pathogenesis model," Math. Biosci. 219, 104–112.
- Wang, X., Elaiw, A. & Song, X. [2012] "Global properties of a delayed HIV infection model with CTL immune response," Appl. Math. Comput. 218, 9405–9414.
- Wang, Y., Brauer, F., Wu, J. & Heffernan, J. M. [2014] "A delay-dependent model with HIV drug resistance during therapy," J. Math. Anal. Appl. 414, 514 - 531.
- Wang, S., Xu, F. & Song, X. [2018] "Thresholds and bistability in HIV infection models with oxidative stress," arXiv preprint arXiv:1808.02276.
- WHO [2020] "HIV/AIDS: Key facts," http://www.who. int/news-room/fact-sheets/detail/hiv-aids.
- Wodarz, D., Christensen, J. P. & Thomsen, A. R. [2002] "The importance of lytic and nonlytic immune responses in viral infections," TRENDS Immunol. 23, 194 - 200.
- Wodarz, D. & Lloyd, A. L. [2004] "Immune responses and the emergence of drug-resistant virus strains in vivo," Proc. R. Soc. Lond. B 271, 1101–1109.
- Yang, Z., Min, Z. & Yu, B. [2020] "Reactive oxygen species and immune regulation," Int. Rev. Immunol. **39**, 292–298.
- Zhang, W., Wahl, L. M. & Yu, P. [2013] "Conditions for transient viremia in deterministic in-host models: Viral blips need no exogenous trigger," SIAM J. Appl. Math. **73**, 853–881.
- Zhang, W., Wahl, L. M. & Yu, P. [2014] "Viral blips may not need a trigger: How transient viremia can arise in deterministic in-host models," SIAM Rev. 56, 127 - 155.